Int. J. Electrochem. Sci., 16 **(2021)** Article ID: 210758, doi: 10.20964/2021.07.33

International Journal of
ELECTROCHEMICAL
SCIENCE
www.electrochemsci.org

Effect of Zn-doping on the Electrochemical Performance of $NaFePO_4$/C Cathode Material for Lithium Ion Battery

Zhe Guo[1], *Xiang Yao*[1,2], *Hualing Tian*[1,2], *Yanjun Cai*[1], *Zhi Su*[1,2,*]

[1] College of Chemistry and Chemical Engineering, Xinjiang Normal University, Urumqi, 830054 Xinjiang, China
[2] Xinjiang Key laboratory of energy storage and photoelectrocatalytic materials, Urumqi, 830054 Xinjiang, China
[*]E-mail: suzhixj@sina.com

Received: 11 March 2021 / *Accepted:* 8 May 2021 / *Published:* 31 May 2021

In this study, we adopted a solid-state method to prepare maricite-$NaFePO_4$ compound cathode material that doped by Zn and coated by carbon. Using XRD and TEM measured the microstructures and surface topography of the material. The results show that the products are crystal structure of $NaFePO_4$, and $NaFe_{1-x}Zn_xPO_4$/C particles with the size of 400-700 nm are coated by 2-3 nm carbon. Electrochemical tests show that the cycling performance and rate capacity of $NaFe_{0.97}Zn_{0.03}PO_4$/C composite are the best of all the materials. $NaFe_{0.97}Zn_{0.03}PO_4$/C demonstrated an preliminary discharge performance of 113.5 mAh·g^{-1} (0.1 C), and retention performance kept at 92% after 50 cycles. The result showed that the discharge capacity of $NaFe_{0.97}Zn_{0.03}PO_4$/C still maintained 50.6 mAh·g^{-1} (2 C). All the results proved that Zn-ion doping can effectively increase the electrochemical performance of $NaFePO_4$/C cathode material.

Keywords: Maricite-$NaFePO_4$; Electrochemical performance; Solid-state method; Cathode material

1. INTRODUCTION

The development and utilization of clean energy can reduce the environmental pollution and consumption of fossil energy. The energy storage device is the key to the conversion and storage of clean energy. Lithium-ion battery (LIBs) is an important capacity storage installation, which is available for computer, electric vehicle and other mobile devices[1-2]. As an important part of LIBs, cathode materials affect the high energy/power density of the LIBs[3]. In order to satisfy the increasing demand of batteries, it is necessary to explore and study the cathode materials. The iron-based phosphates were

low-cost and environment friendly, it is conducive to the wide application of LIBs. In the latest research of iron-based cathode materials, $NaFePO_4$ attracts a lot of attention owing to high theoretical capacity (154 $mAh \cdot g^{-1}$). $NaFePO_4$ is well known to have two structures, olivine $NaFePO_4$ and maricite $NaFePO_4$. Olivine $NaFePO_4$ needs to be prepared by complex ion exchange method, which limits its production and application[4]. The synthetic method of maricite $NaFePO_4$ is simpler than that of olivine $NaFePO_4$. However, the low conductivity of maricite $NaFePO_4$ leads to poor rate performance, and the poor cycle stability of the material, which hinders the application of $NaFePO_4$[5]. In order to overcome the shortcomings of materials, several strategies have been proposed, including reducing particle size, carbon coating and metal ion doping[6].

Generally, maricite $NaFePO_4$ is modified through reducing particle size and incorporating with carbon materials. Liu[7] prepared nanospheres formed by ultra-small $NaFePO_4$ particles (3 nm) uniformly dispersed in the three dimensional carbon network. Liu[8] encapsulated $NaFePO_4$ nanoparticles (≈ 1.6 nm) in porous carbon nanofibers by electrospinning. The composite materials show distinguish electrochemical properties. Nanoparticles can reduce the migration distance of ions/electrons, and enlarge the contact area with electrolyte, while carbon coating can promote charge transfer. Further modification of cathode materials can enhance the electrochemical performance of the battery. Among them, as one of the most feasible methods, metal ion doping can be used to promote the electrochemical capability of electrode materials, the main reason is to raise the intrinsic conductivity and ion diffusion of the electrode materials[9]. Therefore, it has been implemented to modify other sodium based cathode materials. Zhang[10] demonstrate that Ti doping can ameliorate the diffusion of ions. Compared with the pure phase, Ti doped $Na_3V_2(PO_4)_3$ showed better cycle performance. Liu[11] found that Zn doping is beneficial to the ion/electron diffusion of $NaTi_2(PO_4)_3$ materials, thus improving the rate performance of the materials.

Herein, we prepared a series of Zn doping $NaFePO_4$ cathode material through a solid state reaction. Zinc is rich in reserves and cheap, and it has already been used as one of the dopants for modification of cathode materials[12]. Such as, Zn-doping $NaNi_{0.2}Fe_{0.35}Mn_{0.45}O_2$[13], Zn-doping $Na_3Ni_2SbO_6$[14]. On the basis of the above research, this article explored the electrochemical properties strategy of the $NaFePO_4$/C cathode materials for Li^+/Na^+ ion battery which doped by Zinc ion. Meanwhile, the sake of exploring the influence on electrochemical performance by Zn-doping, pure phase was also prepared to compare.

2. EXPERIMENTAL

2.1 Synthesize and characterization of materials

All reagents used to synthesize $NaFe_{1-x}Zn_xPO_4$/C (x = 0.00, 0.01, 0.03, 0.05) are analytically pure without any treatment. Firstly, $Fe(CH_3COO)_2 \cdot 4H_2O$, $NH_4H_2PO_4$, Na_2CO_3, $Zn(CH_3COO)_2$ and $C_6H_8O_7$ were added in the agate ball mill pot according to the stoichiometric ratio with deionized water (25 mL), and then milled for 6 hours. The samples were sintered at 300 ℃ for 4 hours and then calcined

at 600 ℃ for 14 hours in an Ar atmosphere. The black product obtained after calcination was ball-milled at 400 rpm for 18 hours with isopropanol (20 mL) as dispersant. Finally, the sample was dried to obtain $NaFe_{1-x}Zn_xPO_4/C$ composite (x = 0.00, 0.01, 0.03, 0.05).

2.2 Characterization

Utilizing X-ray diffraction (XRD, Bruker D2) to analyze the structures of $NaFe_{1-x}Zn_xPO_4/C$ (x = 0.00, 0.01, 0.03, 0.05). In order to measure and analyze the materials's microscope morphology, we used the transmission electron (TEM, JEOLJEM-2100F).

2.3 Electrochemical tests

The cathode material was placed into cells to test electrochemical performance. Add the active substance and binder polytetrafluor (PVDF) to the mortar according to the mass ratio of 1:1, blend the mixture slurry and applied to the surface of the aluminum foil. Then cut the aluminum foil by the punch with the diameter of 10 mm. The electrode pieces are dried in a vacuum drying oven. Put the battery together in a glove box flowed in Ar. The counter electrodes adopted as the Li sheets, using 1 $mol \cdot L^{-1}$ $LiPF_6$ (EC:DMC:EMC=1:1:1 volume) as the electrolyte, the diaphragm adopted to the thereinto Celgard 2400.

The constant current charge-discharge performance of the material was tested by Wuhan CT2001A Land test system, and the voltage is controlled at 1.5-4.5 V. On the electrochemical workstation (CHI 660E), we has tested the cyclic voltammetry (CV; scan rate= 0.1 $mV \cdot s^{-1}$) and electrochemical impedance (EIS; frequency=0.01-0.1 MHz).

3. RESULTS AND DISCUSSION

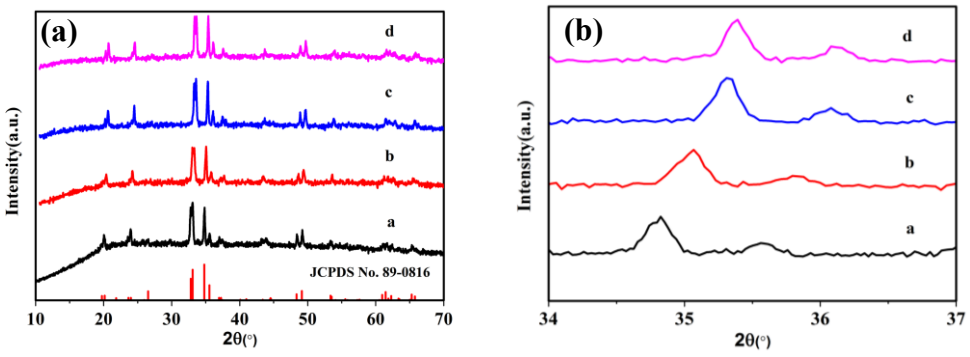

Figure 1. (a) XRD patterns and (b) enlarged (301) peaks of the as-obtained $NaFe_{1-x}Zn_xPO_4/C$ materials (x = 0.00, 0.01, 0.03, 0.05; a, b, c, d, respectively)

XRD patterns of $NaFe_{1-x}Zn_xPO_4/C$ (x = 0.00, 0.01, 0.03, 0.05) was presented in Figure 1a. The diffraction peaks are consistent with the standard card (JCPDS card NO. 89-0816), and no impurity peaks are found, which means that the crystal structure of $NaFePO_4$ is no change when the doping amount is low content[15]. The diffraction peak of the doped material in the figure is sharp, indicating the material has good crystallinity.

Figure 1b is an enlarged view of sample comparison at the peak value of (301). As its content of Zn ions increases, the diffraction peak of Zn doping $NaFePO_4$ shifts to a larger angle position. The reason for this phenomenon is that the radius of Zn^{2+} (r = 74 pm) is smaller than that of Fe^{2+} (r = 78 pm), and the doping of Zn in the host lattice causes the lattice shrinkage of the $NaFePO_4$. This may heighten conductivity, thereby intensifying the charge discharge performance of the $NaFePO_4$ doped by Zn ion[16].

Table 1. Lattice parameters of $NaFe_{1-x}Zn_xPO_4/C$ (x = 0.00, 0.01, 0.03, 0.05) composite material.

Samples (x value)	a(Å)	b(Å)	c(Å)	V(Å^3)
0	9.0936	6.9084	5.0647	318.18
0.01	8.9725	6.9528	5.0828	317.09
0.03	8.9948	6.8634	5.0885	314.14
0.05	8.7659	6.9860	5.0766	312.88

Table 1 shows the lattice parameters of $NaFe_{1-x}Zn_xPO_4/C$(x = 0.00, 0.01, 0.03, 0.05). The results manifest the lattice parameters of pure phase and doping materials are different. The cell volume of Zn^{2+} doping materials is gradually decreased as the increase of the Zn^{2+} ion. The change of cell volume may be caused by the substitution of Zn^{2+} for Fe^{2+}, which proves that Zn was successfully doped into $NaFePO_4$[17].

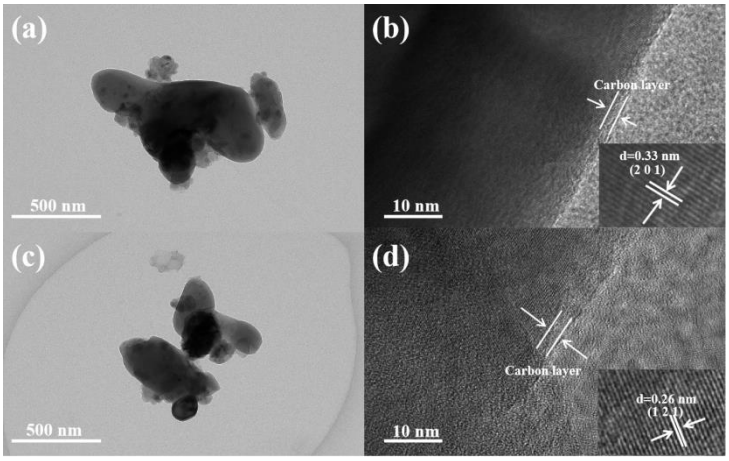

Figure 2. TEM images of samples of $NaFe_{1-x}Zn_xPO_4/C$ (x = 0.00, 0.03). (a) x = 0.00; (c) x = 0.03; HRTEM images of the samples from $NaFe_{1-x}Zn_xPO_4/C$ (x = 0.00, 0.03). (b) x = 0.00; (d) x = 0.03.

Figure 2a and Figure 2c display the TEM diagram of $NaFe_{1-x}Zn_xPO_4/C$ (x = 0.00, 0.03), respectively. It can be found that the morphology of $NaFePO_4$ is not influential by Zn doping. It can be clearly seen that the prepared materials show irregular block structure. The average particle diameter reached as 400-700 nm. Figure 2b and Figure 2d show the HRTEM diagram of $NaFe_{1-x}Zn_xPO_4/C$ (x = 0.00, 0.03), respectively. From the diagram, we can see that the lattice fringes of the samples are relatively clear, implying the samples has the good crystallinity. It makes no difference in comparison to the analysis of XRD. The lattice matches the (201) and (121) faces of $NaFePO_4$ crystal respectively, which is spacing are about 0.33 and 0.26 nm. In addition, a layer of 2-3 nm carbon layer can be seen on the surface of $NaFe_{1-x}Zn_xPO_4/C$ particles, which can inhibit the $NaFePO_4$ particles size growth, providing some ways for electron transfer, and improving the conductivity of the materials. The carbon layer thickness of the samples is close, so the impact on the electrochemical property is different[18].

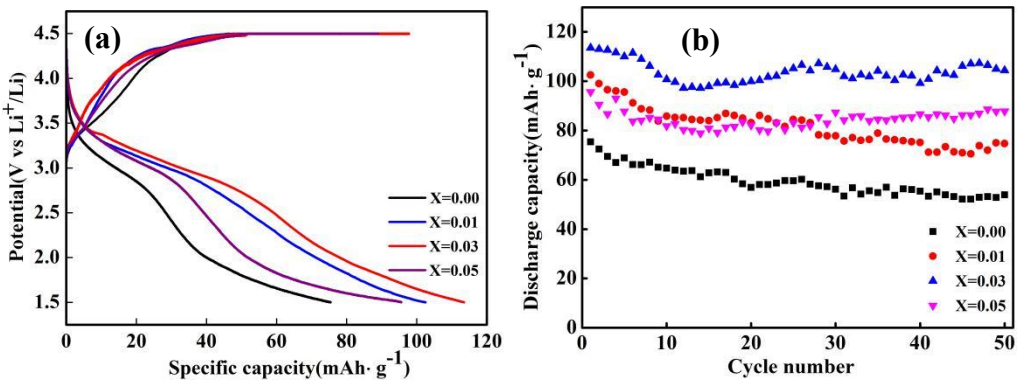

Figure 3. (a) First cycle curves and (b) Cyclic stability of $NaFe_{1-x}Zn_xPO_4/C$ (x = 0.00, 0.01, 0.03, 0.05) materials in the first cycle.

Table 2. Electrochemical performances of iron based phosphates.

Cathode material	Rate	Cycle number	Specific capacity ($mAh \cdot g^{-1}$)	Ref
$NaFe_{0.97}Zn_{0.03}PO_4/C$	0.1 C	50	104.4	our work
$NaFePO_4/C$	0.1 C	50	52	[20]
Na_2FePO_4F	0.1 C	60	67.9	[21]
Na_2FePO_4F/C	0.1 C	30	100.1	[22]
$Na_3FePO_4CO_3/C$	0.05 C	5	68	[23]
$Na_3Fe_2(PO_4)_2F_3$	0.2 C	100	40	[24]

The initial discharge curves of $NaFe_{1-x}Zn_xPO_4/C$ (x = 0.00, 0.01, 0.03, 0.05) are exhibited in Figure 3a. It is obvious that there is no significant voltage plateau in the inclined charge discharge curve, which is in accordance with the published literature[5]. At 0.1 C in the first cycle, When x = 0.00, 0.01, 0.03, 0.05, the discharge capacities of the doped samples are 75.4, 102.5, 113.5, 95.6 $mAh \cdot g^{-1}$, respectively. Among them, $NaFe_{0.97}Zn_{0.03}PO_4/C$ showed the highest discharge capacity (113.5 $mAh \cdot g^{-1}$), which is due to the improvement of conductivity by Zn doping. However, the decrease of

$NaFe_{0.95}Zn_{0.05}PO_4/C$ capacity may be that the amount of Zn doping is too high, so that the lattice distortion caused by Zn doping is too large, leading to the under utilization of active materials[19].

It can be seen from the cyclic stability diagram of $NaFe_{1-x}Zn_xPO_4/C$ (Figure 3b), the ability of $NaFePO_4/C$ is improved after Zn doping. Initial discharge capacity of $NaFe_{0.97}Zn_{0.03}PO_4/C$ electrode is 113.5 $mAh \cdot g^{-1}$. At the end of 50 cycles, it still keeps on 104.4 $mAh \cdot g^{-1}$ at 0.1 C after 50 cycles, which remain the capacity is close to 92%. For comparison, discharge capacity of $NaFePO_4/C$ is only 75.4 $mAh \cdot g^{-1}$, after 50 cycles remain on 53.9 $mAh \cdot g^{-1}$. The retention rate was 71.5% under the same operation. Compared with $NaFePO_4/C$ electrode, the stability of $NaFe_{0.97}Zn_{0.03}PO_4/C$ is better. In addition, as shown in Table 2, $NaFe_{1-x}Zn_xPO_4/C$ shows good electrochemical performance compared with previous studies on iron-based phosphate in lithium batteries. The improvement of cycle stability is mainly because the radius of doped Zn is not variable in the course of charging/discharging process, so Zn doping can stabilize crystal structure of the material[25].

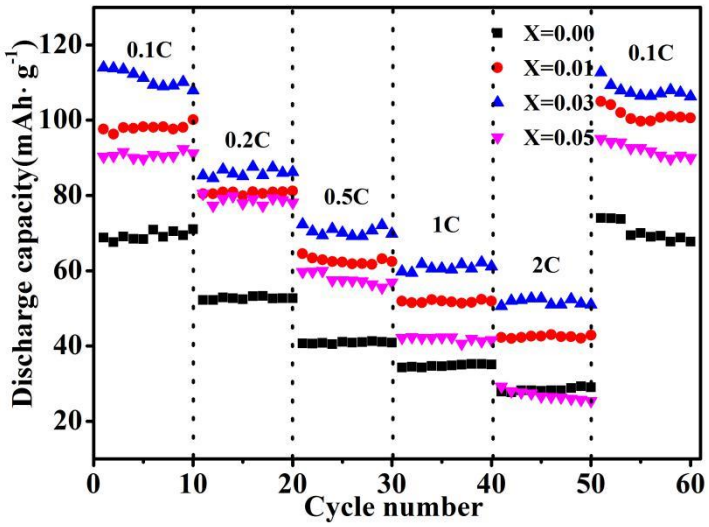

Figure 4. Rate performance of $NaFe_{1-x}Zn_xPO_4/C$ (x = 0.00, 0.01, 0.03, 0.05) samples.

Figure 4 shows the rate performance of $NaFe_{1-x}Zn_xPO_4/C$ (x = 0.00, 0.01, 0.03, 0.05). The samples are tested at 0.1, 0.2, 0.5, 1 and 2 C, respectively. The discharge capacity of Zn doping $NaFe_{1-x}Zn_xPO_4/C$ samples is higher than that of the pure phase. The rate performances of the materials are different with different doping amount of Zn. When x is 0.03, the rate performance of the material is the best. At 0.1, 0.2 and 0.5 C, the discharge capacities of $NaFe_{0.97}Zn_{0.03}PO_4/C$ sample are 114, 85.3 and 72.3 $mAh \cdot g^{-1}$, respectively. Whereas, the $NaFePO_4/C$ sample delivers discharge capacities of 68.8, 52.2 and 40.7 $mAh \cdot g^{-1}$ at the identical conditions. The discharge capacities of the $NaFe_{0.97}Zn_{0.03}PO_4/C$ material can reach 59.8 and 50.6 $mAh \cdot g^{-1}$ in the 1 C and 2 C. Distinctly, doping enables the rate performance of $NaFePO_4/C$ materials. When x is 0.03, the electrochemical performance is the best. The lattice distortion of $NaFePO_4/C$ can be caused by Zn doping, which is beneficial to the conduction of electrons and ions, thus improving the rate properties[26].

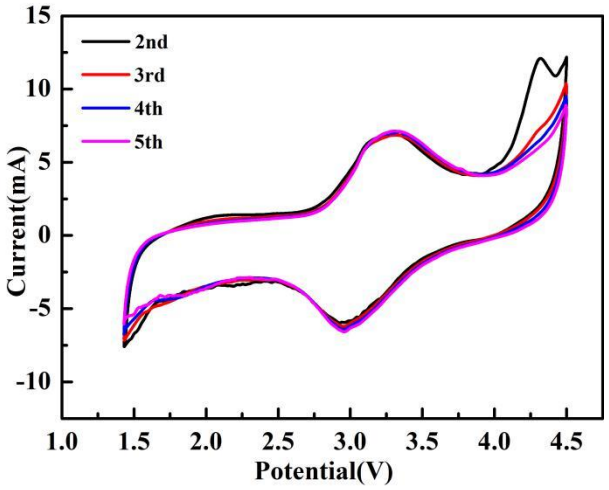

Figure 5. The cyclic voltammetry curves of $NaFe_{0.97}Zn_{0.03}PO_4/C$ sample.

Figure 5 shows the CV curve of $NaFe_{0.97}Zn_{0.03}PO_4/C$ sample. There were two peaks situated on the regions of 2.96 and 3.29 V, which were connected with the redox reaction of Fe^{2+}/Fe^{3+}[27]. In the first three cycles, the CV curves of the samples coincide well, indicating that $NaFe_{0.97}Zn_{0.03}PO_4/C$ sample has good reversibility and stability in the electrochemical process.

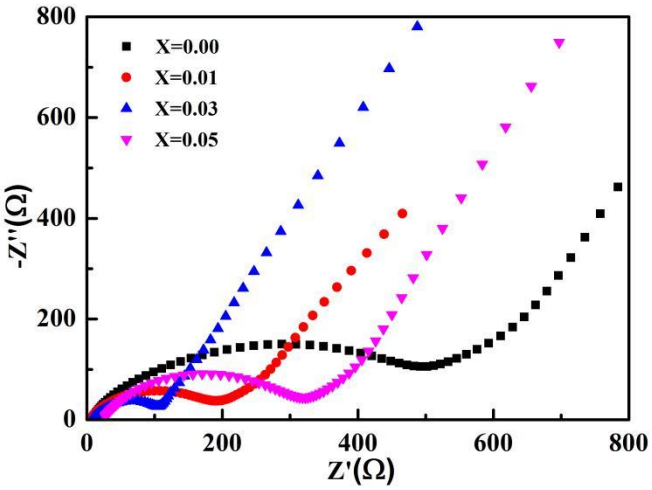

Figure 6. The Electrochemical impedance spectra (EIS) of $NaFe_{1-x}Zn_xPO_4/C$ (x = 0.00, 0.01, 0.03, 0.05) samples.

Figure 6 shows the electrochemical impedance spectra of $NaFe_{1-x}Zn_xPO_4/C$ (x = 0.00, 0.01, 0.03, 0.05) materials. The semi-circle in the high frequency fragment on behalf of the charge transfer impedance (Rct). The slope of the low frequency part is associated with Warburg impedance (Zw). In terms of semicircle diameter, $NaFePO_4/C$ electrode is greater than Zn doping electrode. Among them, $NaFe_{0.97}Zn_{0.03}PO_4/C$ has the lowest Rct, which suggesting Zn doping in $NaFePO_4$ can reduce Rct. It is further proved that the electrochemical performance of $NaFe_{0.97}Zn_{0.03}PO_4/C$ is the best.

4. CONCLUSIONS

In this study, $NaFePO_4$/C and Zn doping $NaFe_{1-x}Zn_xPO_4$/C (x = 0.01, 0.03, 0.05) composites are synthesized through the solid phase method. Under the condition will not deform the crystal structure. The Zn-doping cathode material makes for promoting the electrochemical performance of $NaFePO_4$. Among all the materials, $NaFe_{0.97}Zn_{0.03}PO_4$/C showed a high discharge capacity and favourable rate performance, which can reach 113.5 $mAh \cdot g^{-1}$ and 50.6 $mAh \cdot g^{-1}$ at 0.1 C and 2 C. Besides, at the end of 50 cycles at 0.1 C, the capacity remained at 92%. For $NaFePO_4$/C, the improvement of electrochemical performance originates from the lattice distortion of $NaFePO_4$/C cathode materials caused by Zn^{2+} doping, which is conducive to the conduction of electrons and ions in the materials. Moreover, the Zn^{2+} doping strategy effectively enhance the stability of the materials in the process of battery charging and discharging, which stems from the strengthen of crystal structure stability. This strategy also have great potential applies to other materials.

ACKNOWLEDGEMENT
This study was supported by the Xinjiang National Natural Science Foundation of China (No. 2018D01B30)

References

1. R. H. Wang, S. Q. Wu, F. Zhang, X. Zhao, Z. J. Lin, C. Z Wang and K. M Ho, *Physical Chemistry Chemical Physics*, 22 (2020) 13975.
2. K. Amin, L. J. Mao and Z. X. Wei, *Macromolecular Rapid Communications*, 40 (2019) 1800565.
3. J. L. Li, Y. Wang, J. H. Wu, H. Zhao and H. Liu, *Journal of Alloys and Compounds*, 731 (2018) 864.
4. W. Tang, X. H. Song, Y. H. Du, C. X. Peng, M. Lin, S. B. Xi, B. B. Tian, J. X. Zheng, Y. P. Wu, F. Pan and K. P. Loh, *Journal of Materials Chemistry A*, 4 (2016) 4882.
5. X. D. Ma, J. Y. Xia, X. H. Wu, Z. Y. Pan and P. K. Shen, *Carbon*, 146 (2019) 78.
6. H. J. Tian, X. L. Zhao, J. J. Zhang, M. X. Li and H. B. Lu, *ACS Applied Energy Materials*, 1 (2018) 3497.
7. B. Q. Liu, Q. Zhang, L. Li, L. Y. Zhang, Z. S. Jin, C. G. Wang and Z. M. Su, *Chemical Engineering Journal*, 405 (2021) 126689.
8. Y. C. Liu, N. Zhang, F. F. Wang, X. B. Liu, L. F. Jiao and L. Z. Fan, *Advanced Functional Materials*, 28 (2018) 1801917.
9. H. C. Liu, Y. M. Wang and C. C. Hsieh, *Ceramics International*, 43 (2017) 3196.
10. B. Zhang, T. Zeng, Y. Liu and J. F. Zhang, *RSC Advances*, 8 (2018) 5523.
11. N. Liu, K. Shi, K. X. Ma, Y. Wang, J. F. Chen, J. Zhu, Y. H. Li, Z. X. He, W. Meng, L. Dai and L. Wang, *Ceramics International*, 46 (2020) 19452.
12. X. Y. Ji, Q. F. Lu, E. Y. Guo, D. Li, L. B. Yao, H. Liu and X. L. Li, *Journal of The Electrochemical Society*, 165 (2018) A534.
13. Q. J. Mao, C. Zhang, W. Y. Yang, J. B. Yang, L. M. Sun, Y. M. Hao and X. F. Liu, *Journal of Alloys and Compounds*, 794 (2019) 509.
14. F. Aguesse, J. M. Lopez del Amo, L. Otaegui, E. Goikolea, T. Rojo and G. Singh, *Journal of Power Sources*, 336 (2016) 186.
15. H. Xiao, X. B. Huang, Y. R. Ren, X. Ding, Y. D. Chen and S. B. Zhou, *Solid State Ionics*, 333

(2019) 93.
16. Q. Fan, W. Tai, X. W. Liu, Y. F. Tang and Y. F. Chen, *Journal of Nanoscience and Nanotechnology*, 12 (2012) 3974.
17. W. Su, K. Q. Xu, G. B. Zhong, Z. F. Wei, C. Wang and Y. Z. Meng, *International Journal of Electrochemical Science*, 12 (2017) 6930.
18. X. X. Wang, W. W. Wang, B. C. Zhu, F. F. Qian and Z. Fang, *Frontiers of Materials Science*, 12 (2018) 53.
19. Y. Liu, Y. J. Gu, G. Y. Luo, Z. L. Chen, F. Z. Wu, X. Y. Dai, Y. Mai and J. Q. Li, *Ceramics International*, 46 (2020) 14857.
20. L. Zhao, D. M. Zhou, W. X. Huang, X. Y. Kang, Q. W. Shi, Z. L. Deng, X. W. Yan and Y. B. Yu, *International Journal of Electrochemical Science*, 12 (2017) 3153.
21. L. Sharma, A. Bhatia, L. Assaud, S. Franger and P. Barpanda, *Ionics*, 24 (2018) 2187.
22. D. M. Cui, S. S. Chen, C. Han, C. C. Ai and L. J. Yuan, *Journal of Power Sources*, 301 (2019) 87.
23. N. V. Kosova and A. A. Shindrov, *Ionics*, 25 (2019) 5829.
24. S. C. Manna, P. Sandineni and A. Choudhury, *Journal of Solid State Chemistry*, 295 (2021) 121922.
25. W. H. Wang, J. L. Zhang, Z. Jia, C. S. Dai, Y. F. Hu, J. G. Zhou and Q. F. Xiao, *Physical Chemistry Chemical Physics*, 16 (2014) 13858.
26. H. Y. Ma, B. C. Zhao, J. Bai, K. Z. Li, Z. T. Fang, P. Y. Wang, W. Y. Li, X. B. Zhu and Y. P. Sun, *Journal of The Electrochemical Society*, 167 (2020) 070548.
27. M. Karthik, S. Sathishkumar, R. BoopathiRaja, K. L. Meganathan and T. Sumathi, *Journal of Materials Science: Materials in Electronics*, 31 (2020) 21792